



## Special Feature: Analysis Techniques to Evaluate the Next Generation Electronic Materials

Research Report

### Reliability Analysis of Power Module Components by Synchrotron Radiation X-ray Laminography and Diffraction

Hidehiko Kimura, Masanori Usui, Michiaki Kamiyama, Takashi Asada, Satoshi Yamaguchi, Daigo Setoyama and Toshikazu Satoh

Report received on Jan. 31, 2019

**■ABSTRACT■** The synchrotron radiation X-ray (SR) laminography and diffraction methods were developed to realize non-destructive measurements of internal degradation behavior in intelligent power modules (IPMs). The tracking of fatigue behavior by SR laminography in nano-particle Cu bonding layers of IPM specimens showed that the large aggregated Cu clusters introduced tortuous cracks and crack branching resulting in the lower crack propagation rate, which is expected to lead to longer fatigue life. The laminography measurements during aging showed that the oxidation of the nano-particle Cu was the predominant degradation mode to lower the bonding strength, which was improved by the addition of Bi and Sn. The developed rotational spiral slits system enabled the space-resolved diffraction measurement in the bonding layer of IPM specimens. The internal distribution maps of stresses and strains in IPM will be obtainable with this technique. The SR laminography integrated with the spiral-slits-based diffraction technique will make a powerful tool for the reliability analysis of next-generation IPMs.

**■KEYWORDS■** Reliability, Power Module, Degradation, Thermal Stress, Crack Propagation, Synchrotron Radiation X-ray, Laminography, Diffraction, Spiral Slits System, Nanoparticle Bonding

#### 1. Introduction

In order to contribute to realization of the sustainable society, it is important to reduce CO<sub>2</sub> emission from automobiles by “electrification”, replacement of conventional engines with electric vehicles powertrains.<sup>(1-3)</sup> One of the key components of the electric powertrains is the intelligent power module (IPM). It controls electricity between batteries and motors, determining the environmental and driving performances of electric vehicles, hybrid electric vehicles and fuel cell vehicles. The reliability of IPMs is important for those vehicles to be adopted widely in the society.

An IPM is composed of various materials bonded such as a semiconductor device, bonding layers, metal wiring, ceramic substrates and a cooler. The difference of the coefficients of thermal expansion of the materials, surrounding environmental change and the Joule heat produced during the operation result in the degradation and yield of thermal stresses in the IPM. Among the constituent materials, the bonding layers are considered to be influential to the

reliability because they determine the stresses acting on the semiconductor device directly bonded. For Si semiconductor devices widely used today, lead-free solder is mostly used as the bonding layer. For SiC devices that enable operation at higher frequencies and temperatures resulting in higher output power densities,<sup>(4-6)</sup> sintered nano-particle copper is one of the candidates as high-temperature bonding layers.<sup>(7-15)</sup>

“Morphology”, “Stress” and “Microstructure” are the three key points of reliability analysis as illustrated in **Fig. 1**. Based on fracture mechanics, the remaining life of a damaged module with a crack is calculated from a crack driving parameter such as the stress intensity factor,  $K$ , defined as  $K = \sigma(\pi a)^{0.5}F$ , where  $\sigma$  is the stress,  $a$  is the crack length and  $F$  is the material’s constant. The  $\sigma$ ,  $a$  and  $F$  can be obtained basically from “Stress”, “Morphology” and “Microstructure” measurements respectively.

Most of conventional techniques for reliability analysis, such as scanning electron microscopy, are conducted on sample surfaces, enabling detailed investigation on the damage mechanism at microscopic scale.<sup>(16-18)</sup> For the internal investigation of an IPM based

on those techniques, a small sample must be extracted from the inside. The destruction of an IPM makes it difficult to track the internal degradation process and to measure the actual internal stress distribution. The tracking of the process is necessary to obtain the crack propagation rate, i.e. crack speed, which enables the calculation of the remaining life with the measured actual stresses acting on the crack. Therefore, it is necessary to develop the non-destructive measurement techniques based on synchrotron radiation X-ray (SR) for the reliability analysis of IPMs.

In order to conduct the microscopic measurements of these values in a module, SR with significantly higher brilliance and transmissivity than commercial X-ray devices is useful. The SR laminography, a type of computed tomography applicable to large components, is suitable to obtain the internal morphology of cracks and voids.<sup>(19-23)</sup> For the reliability analysis of IPMs where the internal voids and microstructures need to be visualized at the scale of 1  $\mu\text{m}$ , the SR with significantly high brilliance and transmissivity is necessary instead of commercial devices without sufficient X-ray. The SR diffraction methods enable the internal microstructure measurement based on three-dimensional X-ray diffraction microscopy (3DXRD),<sup>(24-27)</sup> as well as the internal stress measurement.

In this study, SR laminography and diffraction methods were developed to realize non-destructive measurements of internal degradation behavior in IPMs. The fatigue and aging mechanisms in the bonding layer consisting of nano-particle Cu were investigated by SR laminography.<sup>(28-29)</sup> The diffraction measurement from the internal bonding layer was enabled by a developed rotational spiral slits system.<sup>(30)</sup>

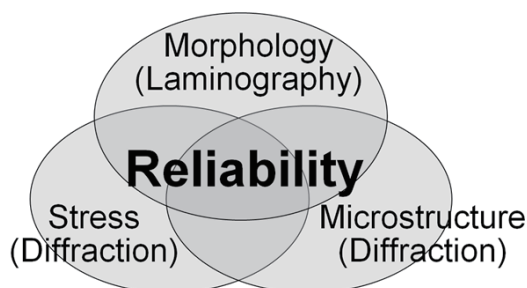


**Fig. 1** Schematic of three key points for reliability analysis.

## 2. Specimens and Methods

### 2.1. Laminography for Internal Degradation Morphology Measurement

Specimens with similar structure to that of the IPMs were prepared. Semiconductor chips were bonded on Al substrate of direct bonded aluminum (DBA), with aluminum nitride (AlN) plate between the Al layers. For the investigation of thermal fatigue degradation, Si chips were bonded by nano-particle Cu on the DBA substrates based on the developed sintering process as illustrated in **Fig. 2**.<sup>(28)</sup> The specimens were fatigued under repeated thermal stress cycles between  $-40^{\circ}\text{C}$  and  $150^{\circ}\text{C}$  with each exposure time of 30 min in air at 1 atm.

For the investigation of high-temperature aging degradation, SiC chips were bonded by the sintered nano-particle Cu containing Bi and Sn as well as Cu.<sup>(29)</sup> The specimens were subjected to thermal aging at  $225^{\circ}\text{C}$  for 100 hour in air at 1 atm.

The SR experiments were conducted at the beamline of BL33XU (Toyota beamline) of SPring-8,<sup>(31,32)</sup> large synchrotron radiation facility in Japan. **Figure 3** shows a schematic of the experimental setup of SR laminography compared with the conventional computed tomography (CT). As shown in Fig.3 (a), a small sample must be extracted from the bonding layer with low transmissivity in the case of conventional CT measurement to obtain the transmission images. The maximum diameter of the extracted sample is about 1 mm for Cu or solder measured at SR energy of 30 keV. The destruction of the specimen makes it difficult to track the internal degradation process that is influenced by the bonded structure. On the other hand, the full-size component

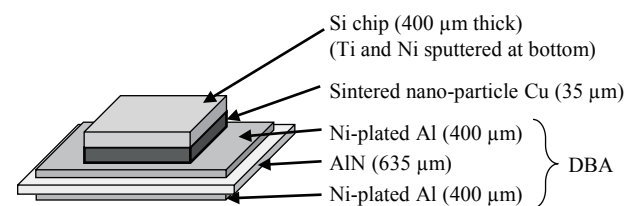


**Fig. 2** Schematic of specimen with similar structure to power module for thermal fatigue degradation investigation by SR laminography.

can be measured by SR laminography as shown in Fig. 3 (b). The tilted specimen rotational axis reduces the transmission distance of SR beam compared with the width of the full-size module, hundreds of mm, that must be transmitted in the case of conventional CT setup. In order to realize the measurement of full-size modules, a high-rigidity rotation stage was developed with high-precision positioning algorithm. Hence, the SR laminography at BL33XU of SPring-8 is suitable for the non-destructive internal measurement of full-size modules, enabling the tracking of the internal degradation behavior.

In this study, the specimen rotation axis was tilted at an angle of  $60^\circ$  with respect to the SR beam. The transmitted SR was converted into visible light by a scintillator and captured by a CCD camera through magnification lenses that yield the voxel size of

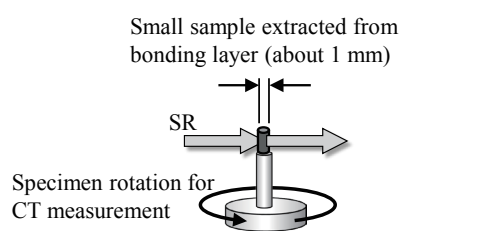
$0.33$  or  $1.3 \mu\text{m}$ . The specimens were rotated  $360^\circ$  while 3600 transmission images were captured with each exposure time of 0.1 second. The 3-dimensional image reconstruction was conducted based on a filtered back-projection method for the setup of the tilted sample rotation axis.<sup>(19)</sup> The energy of SR was set to 29 keV so that it can transmit the specimens. The SR laminography measurements were carried out before the fatigue and aging. The same positions were measured again after the fatigue test of 500 cycles and the aging of 100 hours. The degradation behaviors were then compared.

## 2.2. Diffraction Technique for Internal Stress Measurement

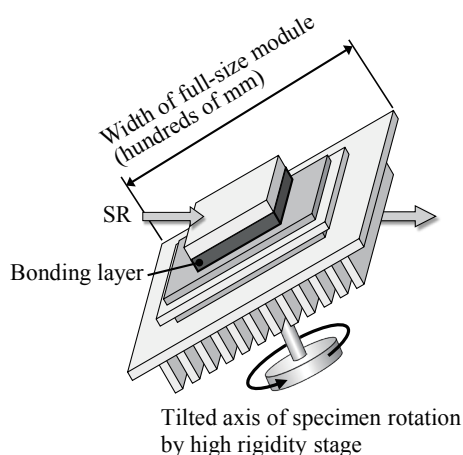
The specimen for the diffraction measurement of the bonding layer consists of a Si chip bonded by lead-free solder on a DBA substrate.

Strains are obtained from the change of the SR diffraction patterns between non-stressed and stressed conditions. Stresses can then be calculated from components of strains. High energy SR that deeply penetrates through a specimen enables the strain measurement inside of an IPM. The incident SR beam is narrowed to obtain high-resolution strain distribution map. The diffraction pattern from the small gauge volume, i.e. measurement point, is spotty because the number of the grains inside of the volume is too small to yield the continuous diffraction rings. An area detector is necessary to capture the discrete diffraction spots instead of the conventional point or linear detectors. In order to measure diffraction from inside of a specimen with an area detector, a special type of slits system is indispensable as shown in Fig. 4. Though conventional double slits in Fig.4 (a) shields diffracted SR beam from positions out of the gauge volume, most of area on the detector is also shielded by the shadow of the slits. With only limited diffraction, strain measurement is difficult. On the other hand, two-dimensional spiral slits system in Fig.4 (b) allows all diffracted beams from the gauge volume to reach the area detector when the slits are rotated, while the diffraction out of the gauge volume is shielded by the slits. Thus, this spiral slits system is indispensable to measure the microscopic distribution of internal stress/strain in a large specimen such as an IPM.

The diffraction experiments were performed with



(a) Conventional CT measurement requiring sample extraction from bonding layer with low X-ray transmissivity



(b) Laminography suitable for non-destructive measurement of internal bonding layer in full-size module

**Fig. 3** Schematic of experimental setup for SR laminography compared with conventional computed tomography.

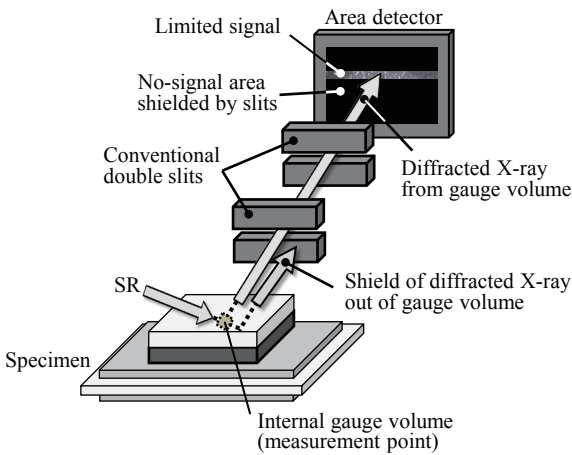
the developed spiral slits system installed at BL33XU of SPring-8. The energy of SR was set to 29 keV for the measurement of the solder bonding layer in the specimen with the width of the incident SR beam and the slits of 50  $\mu\text{m}$ .

### 3. Results and Discussions

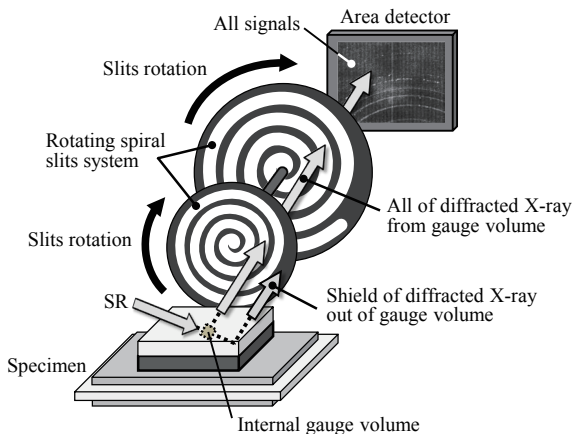
#### 3.1. Internal Degradation Mechanism

Figure 5 shows the 3-dimensional reconstructed images of the nano-particle Cu bonding layer in the specimen. The dark areas in the images indicate

low-density Cu or the presence of pores/light materials, while the bright areas indicate high-density Cu or heavy materials. The SR laminography measurements have enabled the tracking of the degradation behavior during the fatigue cycles at the same position. The image in Fig.5 (a) is at the initial condition, while Fig.5 (b) is the image after 500 thermal fatigue cycles. Though each nano-particle is not visualized because of the grain size less than the measurement resolution of 1.3  $\mu\text{m}/\text{voxel}$ , the clusters of nano-particles are distinguishable as bright aggregates from the dark nano-particle matrix. The average density of the aggregated nano-particle Cu clusters is considered to be higher than the matrix that includes micro pores and organic residue of nano-particle paste. After fatigue cycles in Fig.5 (b), internal cracks are introduced in the bonding layer. Crack branching is observed mainly at the location of the clusters. The crack propagation rate is estimated to be larger in the matrix with low-density nano-particles than in the high-density clusters. When a crack in the matrix propagates close to a cluster, the

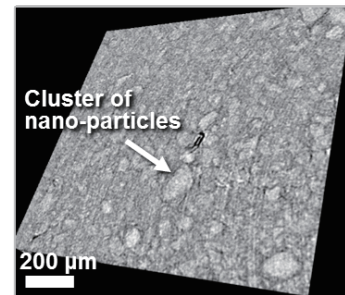


(a) Conventional double slits inapplicable to diffraction measurement with area detector due to shield on detector

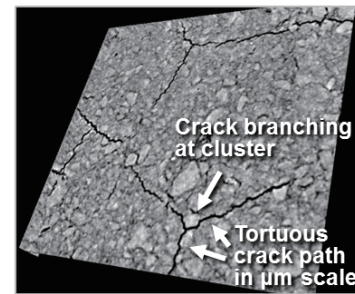


(b) Rotational spiral slits system for diffraction measurement from internal gauge volume with area detector

Fig. 4 Measurement of SR diffraction from inside of specimen by area detector.



(a) Initial internal condition



(b) After 500 thermal fatigue cycles

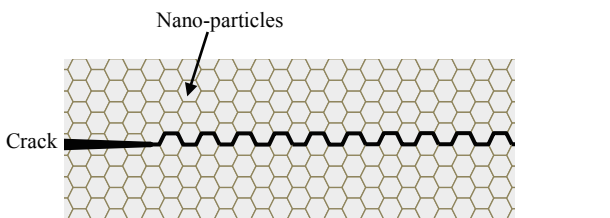
Fig. 5 Reconstructed 3-dimensional images of nano-particle Cu bonding layer before and after thermal fatigue measured by SR laminography.

crack tip is considered to be blocked, resulting in the crack branching avoiding the cluster.

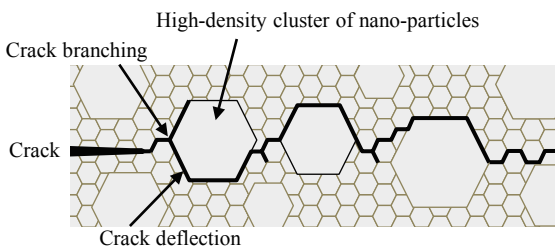
Fatigue crack propagation behavior is significantly influenced by the microstructure of the material. When a long fatigue crack propagates through a material with large grains, the crack path tends to be tortuous at the grain scale forming the rough fracture surface. The crack propagation rate is low due to the roughness-induced crack closure that leads to longer fatigue life. On the other hand, when the propagation is through a material with nano-particles as in **Fig. 6 (a)**, the crack path tends to be smooth forming the relatively flat fracture surface. The resultant crack propagation rate is higher. In the developed nano-particle bonding layer, however, tortuous crack path at the scale of micrometer is observed in spite of the nanometer particles as in Fig. 5 (b). This behavior is attributed to the crack deflection at the scale of the clusters as shown in Fig. 6 (b) as well as the above-mentioned crack branching at the clusters. The crack propagation rate is expected to be lower because of the roughness-induced crack closure caused by the crack branching and deflection. The unique microstructure with the mixture

of nano-particle matrix and the larger rigid clusters is expected to contribute to the longer fatigue life. Thus, the microstructure of the nano-particle Cu bonding layer is considered to have significant influence on the reliability.

**Figure 7** shows the internal cross-sectional images of the 3-dimensional reconstruction from the nano-particle Cu bonding layer before and after aging at 225°C for 100 hour at the same position. The small cracks observed at the initial condition in Fig. 7 (a) are considered to be introduced due to the difference in

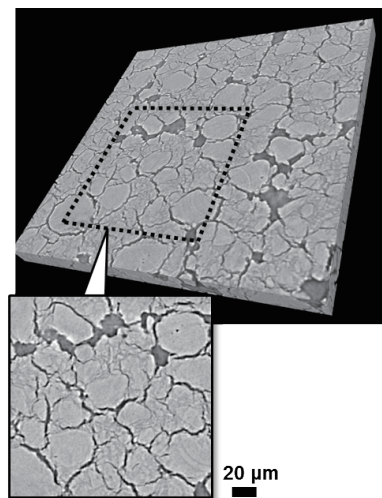


(a) Crack propagation in conventional nano-particle material (Higher crack propagation rate due to flat crack path)

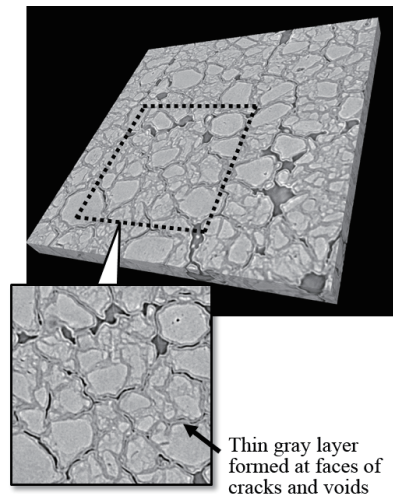


(b) Crack propagation in nano-particle material containing large high-density clusters of nano-particles (Lower crack propagation rate due to tortuous crack path)

**Fig. 6** Schematic of crack propagation behavior in nano-particle Cu bonding layer.



(a) Initial internal condition



(b) After aging at 225°C for 100 hour

**Fig. 7** Reconstructed internal cross-sectional images of nano-particle Cu bonding layer before and after aging measured by SR laminography.

the coefficients of thermal expansion of the SiC chip and DBA substrate. In Fig. 7 (b), the laminography measurement after the aging shows the formation of thin gray layer on the crack faces, resulting in the apparent closure of the small cracks. A post elemental analysis by a scanning electron microscope shows that the gray layer is oxidized Cu that is predominantly observed in low-density Cu area as well as at the faces of the residual cracks and voids. The laminography measurements show that the oxidation of the nano-particle Cu is the predominant degradation mode for the lower bonding strength under aging.

The bonding strength of the developed bonding layer with addition of Bi and Sn to Cu was higher than the one without the addition. The improvement is attributed to the existence of Bi and Sn that are liquid-phase during the sintering process (200°C for 10 min followed by 350°C for 5 min in H<sub>2</sub> under 0.5 MPa) promoting the densification of Cu. In high-density Cu area, the oxidation as well as crack initiation is suppressed. The addition of Bi and Sn is expected to improve the high-temperature strength of the nano-particle Cu bonding layer.

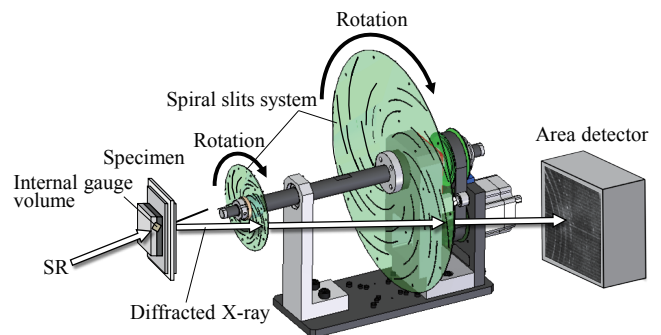
The tracking of internal degradation behavior by SR laminography is also useful to find the fracture origin by tracking back the process from the final crack to the origin.

### 3.2. Diffraction Measurement of Internal Gauge Volume

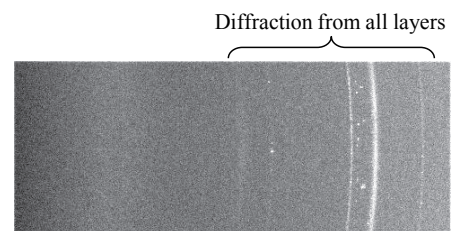
The developed rotational spiral slits system is shown in Fig. 8. The slits in the unique shape of spirals are machined on the shielding disks. The small front disks and large rear disks are connected by a rod with a collimator on the center axis. The shielding disks with the spiral slits are rotated during the diffraction measurement so that the diffracted SR beam only from the internal gauge volume reaches the area detector. The rotation is necessary to capture all of the diffracted SR on the whole area of the detector without the shield by the shielding disks. This rotational spiral slits system is a unique tool that enables measurement of internal stress/strain for each material such as coarse-grained bonding materials, highly textured wiring materials as well as semiconductors.

Figure 9 shows the diffraction patterns obtained from the inside of the specimen with lead-free solder bonding layer. In the measurement without the spiral

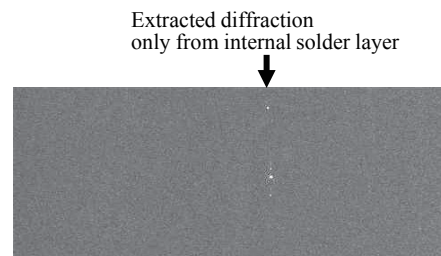
slits system in Fig. 9 (a), many diffraction patterns are observed from various depth positions as well as various materials in the specimen. It is difficult to distinguish the diffraction of the bonding layer from those of the other layers such as Al or AlN. In addition, the position of a diffraction pattern on the detector shifts when the measurement point shifts. This means that, without the spiral slits system, diffraction from a position outside of the gauge volume appears to be the shifted diffraction from the gauge volume, resulting in the misled pseudo strain. On the other hand, the



**Fig. 8** Developed rotational spiral slits system for diffraction measurement from internal gauge volume.



(a) Without rotational spiral slits system



(b) With rotational spiral slits system

**Fig. 9** Diffraction patterns obtained from inside of specimen (Center of detector extracted, contrast adjusted).

diffraction only from the bonding layer is extracted in Fig. 9 (b) in the measurement with the spiral slits system. Since the gauge volume is precisely defined in the specimen by the slits, the strains can be calculated from the shift of the diffraction pattern compared with the one under no stress such as the powder. This diffraction measurement technique with the developed rotational spiral slits system will enable us to obtain internal distribution maps of stresses and strains by scanning the sample such as an IPM.

#### 4. Conclusion

The SR laminography and diffraction methods were developed to realize non-destructive measurements of internal degradation behavior in IPMs. The tracking of fatigue behavior by SR laminography in nano-particle Cu bonding layers of IPM specimens showed that the large aggregated Cu clusters introduced tortuous cracks and crack branching resulting in the lower crack propagation rate, which is expected to lead to longer fatigue life. The laminography measurements during aging showed that the oxidation of the nano-particle Cu was the predominant degradation mode to lower the bonding strength, which was improved by the addition of Bi and Sn. The developed rotational spiral slits system enabled the space-resolved diffraction measurement in the bonding layer of IPM specimens. The internal distribution maps of stresses and strains in IPM will be obtainable with this technique. The SR laminography integrated with the spiral-slits-based diffraction technique will make a powerful tool for the reliability analysis of next-generation IPMs.

#### Acknowledgements

The synchrotron radiation experiments were performed at the BL33XU (Toyota beamline) of the SPring-8 facility with the approval of the Japan Synchrotron Radiation Research Institute (JASRI) (Proposal No. 2015A7012, 2015B7012, 2016A7012 and 2016B7012). The authors would like to thank Dr. M. Hoshino, Dr. K. Uesugi and Dr. K. Kajiwara of JASRI for their support during the previous SR laminography measurements and Dr. T. Shobu of JAEA and Prof. K. Suzuki of Niigata University for their advices about the spiral slits.

#### References

- (1) Ohashi, H., Omura, I., Matsumoto, S., Sato, Y., Tadano, H. and Ishii, I., "Power Electronics Innovation with Next Generation Advanced Power Devices", *IEICE Trans. Commun.*, Vol. 87, No. 12 (2004), pp. 3422-3429.
- (2) Kitazawa, O., Kikuchi, T., Nakashima, M., Tomita, Y., Kosugi, H. and Kaneko, T., "Development of Power Control Unit for Compact-class Vehicle", *SAE Int. J. Alt. Power.*, Vol. 5, No. 2 (2016), pp. 278-285.
- (3) Hasegawa, T., Imanishi, H., Nada, M. and Ikogi, Y., "Development of the Fuel Cell System in the Mirai FCV", *SAE Tech. Pap. Ser.*, No. 2016-01-1185 (2016).
- (4) Hamada, K., Nagao, M., Ajioka, M. and Kawai, F., "SiC—Emerging Power Device Technology for Next-generation Electrically Powered Environmentally Friendly Vehicles", *IEEE Trans. Electron. Devices*, Vol. 62, No. 2 (2015), pp. 278-285.
- (5) Sugiura, T., Tanida, A. and Tamura, K., "Efficiency Improvement of Boost Converter for Fuel Cell Bus by Silicon Carbide Diodes", *SAE Int. J. Alt. Power.*, Vol. 5, No. 2 (2016), pp. 294-298.
- (6) Ogawa, T., Tanida, A., Yamakawa, T. and Okamura, M., "Verification of Fuel Efficiency Improvement by Application of Highly Effective Silicon Carbide Power Semiconductor to HV Inverter", *SAE Tech. Pap. Ser.*, No., 2016-01-1230 (2016).
- (7) Ishizaki, T., Akedo, K., Satoh, T. and Watanabe, R., "Pressure-free Bonding of Metallic Plates with Ni Affinity Layers using Cu Nanoparticles", *J. Electron. Mater.*, Vol. 43, No. 3 (2014), pp. 774-779.
- (8) Satoh, T., Akedo, K. and Ishizaki, T., "X-ray Photoelectron Spectroscopic Study of the Formation of Cu/Ni Interface Mediated by Oxide Phase", *J. Alloys Compd.*, Vol. 582 (2014), pp. 403-407.
- (9) Satoh, T. and Ishizaki, T., "Enhanced Pressure-free Bonding Using Mixture of Cu and NiO Nanoparticles", *J. Alloys Compd.*, Vol. 629 (2015), pp. 118-123.
- (10) Ishizaki, T., Satoh, T., Kuno, A., Tane, A., Yanase, M., Osawa, F. and Yamada, Y., "Thermal Characterizations of Cu Nanoparticle Joints for Power Semiconductor Devices", *Microelectron. Reliab.*, Vol. 53, No. 9-11 (2013), pp. 1543-1547.
- (11) Ishizaki, T., Kuno, A., Tane, A., Yanase, M., Osawa, F., Satoh, T. and Yamada, Y., "Reliability of Cu Nanoparticle Joint for High Temperature Power Electronics", *Microelectron. Reliab.*, Vol. 54, No. 9-10 (2014), pp. 1867-1871.
- (12) Ishizaki, T., Usui, M. and Yamada, Y., "Thermal Cycle Reliability of Cu-nanoparticle Joint", *Microelectron. Reliab.*, Vol. 55, No. 9-10 (2015), pp. 1861-1866.

- (13) Ishizaki, T., Yanase, M., Kuno, A., Satoh, T., Usui, M., Osawa, F. and Yamada, Y., "Thermal Simulation of Joints with High Thermal Conductivities for Power Electronic Devices", *Microelectron. Reliab.*, Vol. 55, No. 7 (2015), pp. 1060-1066.
- (14) Ishizaki, T., Patent No. 5850320 (in Japanese).
- (15) Sato, T., Ishizaki, T. and Usui, M., Unexamined Patent Pub. 2017-101313 (in Japanese).
- (16) Kimura, H., Akiniwa, Y., Tanaka, K., Kondo, J. and Ishikawa, T., "Effect of Microstructure on Fatigue Crack Propagation Behavior in Ultrafine-grained Steel", *J. Soc. Mater. Sci., Jpn.* (in Japanese), Vol. 51, No.7 (2002), pp. 795-800.
- (17) Kimura, H., Akiniwa, Y., Tanaka, K., Tahara, Y. and Ishikawa, T., "Fatigue Crack Initiation Behavior in Ultrafine-grained Steel Observed by AFM and EBSP", *JSME Int. J., Ser. A*, Vol. 47, No. 3 (2004), pp. 331-340.
- (18) Kojima, Y., Kimura, H., Akiniwa, Y. and Ju, Y., "Microscopic Analysis by EBSD Method on Fatigue Crack Propagation Behaviour in Ultrafine-grained Copper", *Trans. Jpn. Soc. Mech. Eng., Ser. A* (in Japanese), Vol. 75, No. 754 (2009), pp. 742-751.
- (19) Hoshino, M., Uesugi, K., Takeuchi, A., Suzuki, Y. and Yagi, N., "Development of an X-ray Micro Laminography System at SPring-8", *AIP Conf. Proc.*, Vol. 1365 (2011), pp. 250-253.
- (20) Hoshino, M., Uesugi, K., Takeuchi, A., Suzuki, Y. and Yagi, N., "Development of X-ray Laminography under an X-ray Microscopic Condition", *Rev. Sci. Instrum.*, Vol. 82 (2011), 073706.
- (21) Hoshino, M., Uesugi, K., Takeuchi, A., Suzuki, Y. and Yagi, N., "Three-dimensional Structural Analysis of Laterally Extended Objects Using X-ray Laminography", *J. Jpn. Soc. Synchrotron Radiat. Res.* (in Japanese), Vol. 26, No. 5 (2013), pp. 257-267.
- (22) Kimura, H., Asada, T., Yamaguchi, S., Kano, T., Hoshino, M. and Uesugi, K., "Nondestructive Measurement of Discontinuous Deformation at Internal Interfaces of Power Device Package", *SPring-8/SACLA Res. Rep.* (in Japanese), Vol. 3 (2015), pp. 50-52.
- (23) Asada, T., Kimura, H., Yamaguchi, S., Hayashi, Y. and Uyama, T., "Measurement of 3-dimensional Internal Strain Field in Power Module Package by Synchrotron Laminography and Volumetric Digital Image Correlation Method", *Proc. Int. Conf. Adv. Technol. Exp. Mech.*, Vol. 2015.14 (2015), p. 48.
- (24) Hayashi, Y., Hirose, Y. and Setoyama, D., "In Situ Three-dimensional Orientation Mapping in Plastically-deformed Polycrystalline Iron by Three-dimensional X-ray Diffraction", *Mater. Sci. Forum*, Vol. 777 (2014), pp. 118-123.
- (25) Hayashi, Y., Hirose, Y. and Seno, Y., "Polycrystal Orientation Mapping Using Scanning Three-dimensional X-ray Diffraction Microscopy", *J. Appl. Crystallogr.*, Vol. 48 (2015), pp. 1094-1101.
- (26) Setoyama, D., Hayashi, Y. and Iwata, N., "Crystal Plasticity Finite Element Analysis Based on Crystal Orientation Mapping with Three-dimensional X-ray Diffraction Microscopy", *Mater. Sci. Forum*, Vol. 777 (2014), pp. 142-147.
- (27) Hayashi, Y., Setoyama, D. and Seno, Y., "Scanning Three-dimensional X-ray Diffraction Microscopy with a High-energy Microbeam at SPring-8", *Mater. Sci. Forum*, Vol. 905 (2017), pp. 157-164.
- (28) Usui, M., Kimura, H., Satoh, T., Asada, T., Yamaguchi, S. and Kato, M., "Degradation of a Sintered Cu Nanoparticle Layer Studied by Synchrotron Radiation Computed Laminography", *Microelectron. Reliab.*, Vol. 63 (2016), pp. 152-158.
- (29) Usui, M., Satoh, T., Kimura, H., Tajima, S., Hayashi, Y., Setoyama, D. and Kato, M., "Effects of Thermal Aging on Cu Nanoparticle/Bi-Sn Solder Hybrid Bonding", *Microelectron. Reliab.*, Vol. 78 (2017), pp. 93-99.
- (30) Setoyama, D. and Kimura, H., Patent No. 6217400 (in Japanese).
- (31) Nonaka, T., Dohmae, K., Hayashi, Y., Araki, T., Yamaguchi, S., Nagai, Y., Hirose, Y., Tanaka, T., Kitamura, H., Uruga, T., Yamazaki, H., Yumoto, H., Ohashi, H. and Goto, S., "Toyota Beamline (BL33XU) at SPring-8", *AIP Conf. Proc.*, Vol. 1741, No. 1 (2016), 030043.
- (32) Hirose Y., "Toyota Beamline BL33XU", *SPring-8 Research Frontiers* (2009), p. 170, SPring-8/JASRI.

**Hidehiko Kimura**

Research Field:

- Reliability Analysis Based on Micro Fracture Mechanics and Applied Quantum Beam Measurements

Academic Degree: Ph.D

Academic Societies:

- The Japan Society of Mechanical Engineers
- The Society of Materials Science, Japan

Awards:

- Young Engineers Award, The Japan Society of Mechanical Engineers, 2004
- Award for Promising Reserchers, The Society of Materials Science, Japan, 2008
- Best Paper Award, The Japan Institute of Electronics Packaging, 2017

**Satoshi Yamaguchi**

Research Field:

- Advanced Imaging Technique by Synchrotron Radiation

Academic Society:

- The Japanese Society for Synchrotron Radiation Research

**Masanori Usui**

Research Field:

- Reliability Analysis of Power Devices and Modules

Academic Degree: Dr.Eng.

Academic Society:

- The Japan Institute of Electronics Packaging

Award:

- Best Paper Award, Micro Electronics Symposium, 2016

**Daigo Setoyama**

Research Field:

- Reliability Analysis Based on Micro Fracture Mechanics and Applied Quantum Beam Measurements

Academic Degree: Ph.D

Academic Societies:

- The Japan Society of Mechanical Engineers
- The Society of Materials Science, Japan
- The Japan Institute of Metals and Materials

Award:

- Best Paper Award, The Atomic Energy Society of Japan, 2003

**Michiaki Kamiyama**

Research Field:

- Reliability Analysis Based on Quantum Beam Measurement and Machine Learning

**Toshikazu Satoh**

Research Field:

- Materials Science in Electronics Packaging

Academic Societies:

- The Japan Institute of Electronics Packaging
- The Japan Society of Applied Physics

Award:

- Best Paper Award, Microelectronics Symposium, 2016

**Takashi Asada**

Research Fields:

- Dissimilar Metals Joining
- Hydrogen Embrittlement

Academic Degree: Ph.D.

Academic Society:

- The Japan Society of Mechanical Engineers

Award:

- Young Engineers Award, The Japan Society of Mechanical Engineers, 2016

